

15. P. L. Anelli, N. Spencer, J. F. Stoddart, *J. Am. Chem. Soc.* **113**, 5131 (1991).
16. J.-P. Sauvage, C. Dietrich-Buchecker, Eds., *Molecular Catenanes, Rotaxanes and Knots* (VCH-Wiley, Weinheim, Germany, 1999).
17. Y. Luo *et al.*, *ChemPhysChem* **3**, 519 (2002).
18. M.-V. Martínez-Díaz, N. Spencer, J. F. Stoddart, *Angew. Chem. Int. Ed.* **36**, 1904 (1997).
19. S. J. Cantrill, A. R. Pease, J. F. Stoddart, *J. Chem. Soc. Dalton Trans.* **21**, 3715 (2000).
20. M. Mammen, S.-K. Choi, G. M. Whitesides, *Angew. Chem. Int. Ed. Engl.* **37**, 2754 (1998).
21. V. Balzani *et al.*, *Chem. Eur. J.* **9**, 5348 (2003).
22. S. Anderson, H. L. Anderson, J. K. M. Sanders, *Acc. Chem. Res.* **26**, 469 (1993).
23. P. M. S. Monk, *The Viologens. Physicochemical Properties, Synthesis and Application of the Salts of 4,4'-Bipyridine* (Wiley, Chichester, UK, 1998).
24. Although multivalency is a concept that is well-established with regard to numerous biological

systems, its investigation has been restricted largely to the acquisition of thermodynamic parameters, e.g., association or dissociation constants and free energies, enthalpies, and entropies of complexation. In the present investigation, the opportunity arose to study within a molecularly constrained environment how three equivalent recognition sites respond to being addressed chemically. The fact that they switch in series rather than in parallel is a feature worthy of note. Although many might argue intuitively that multivalency from a mechanistic standpoint has to be a stepwise process, the results presented in this article provide indirect yet convincing experimental evidence for the one-at-a-time mechanism; i.e., by taking single steps rather than moving in concert, the molecular elevator is more reminiscent of a legged animal than it is of the passenger elevator.

25. This research was supported by NSF (CHE-0317170, CHE-9974928, and CHE-0116853) in the

United States and the University of Bologna (Funds for selected topics), Ministero dell'Istruzione, dell'Università e della Ricerca (Supramolecular devices project), Fondo per gli Investimenti della Ricerca di Base (RBNE019H9K) and the European Union (Molecular-Level Devices and Machines Network HPRN-CT-2000-00029) in Italy. We thank M. Venturi and P. Ceroni for useful discussions.

Supporting Online Material

www.sciencemag.org/cgi/content/full/303/5665/1849/DC1

Materials and Methods

SOM Text

Scheme S1

Figs. S1 and S2

References

17 December 2003; accepted 12 February 2004

Electrical or Photocontrol of the Rotary Motion of a Metallocarborane

M. Frederick Hawthorne,^{1*} Jeffrey I. Zink,¹ Johnny M. Skelton,¹ Michael J. Bayer,¹ Chris Liu,¹ Ester Livshits,² Roi Baer,² Daniel Neuhauser¹

Rotary motion around a molecular axis has been controlled by simple electron transfer processes and by photoexcitation. The basis of the motion is intramolecular rotation of a carborane cage ligand (7,8-dicarbollide) around a nickel axle. The Ni(III) metallocarborane structure is a *transoid* sandwich with two pairs of carbon vertices reflected through a center of symmetry, but that of the Ni(IV) species is *cisoid*. The interconversion of the two provides the basis for controlled, rotational, oscillatory motion. The energies of the Ni(III) and Ni(IV) species are calculated as a function of the rotation angle.

The smallest nanomachines made to date are based on changes in molecular bonding. In biological motors, such as those that power the linear motion of myosin head in muscle contraction (*1*, *2*) or the rotary motion of F₁-adenosine triphosphatase (*3–5*) in bacterial flagella, the hydrolysis energy of the adenosine triphosphate (ATP) to diphosphate reaction creates new bonds that can exert forces that change the shape of the larger molecule and perform work.

Given the existence of biological motors, the interest of chemists in designing molecular motors stems from the challenge not only of making even smaller nanomachines that perform controllable motion (*6*), but also of creating systems that can be powered with light or electrical energy, rather than depending on the delivery of ATP. Linear motors have been developed such as the rotaxane systems (*7–9*), in which a shuttle ring component slides from one physically discrete zone of a rigid rod to another.

¹Department of Chemistry and Biochemistry, University of California, Los Angeles, CA, 90095–1569, USA.

²Department of Chemistry, Hebrew University of Jerusalem, Givat Ram, Jerusalem, Israel.

*To whom correspondence should be addressed. E-mail: mfh@chem.ucla.edu

Assessing a potential molecular motor based on changes in bonding must include determining whether the system has well-defined reactant and product states that are separated by a considerable energy barrier. The reasons are twofold. First, there has to be some way of putting into the molecule energy that will be recovered later as work. For photon-driven systems, this would likely be an excited state; for electrically driven systems, this could be the formation of an intermediate with a different redox state. Second, in either case, the product formed must have a barrier against back reaction, or it is unlikely that the system would exert any force; it would more likely relax back unproductively to the reactant configuration.

With these configurations in mind, we reexplored a small metal complex with potential as a two-state rotary machine that could be used, for example, to open or close a valve or switch. Examples to date of artificial rotors have been few. Rotary motion in synthetic arrays is represented by molecular windmills and turnstiles in which one component of the molecular device is capable of freewheeling rotation on a molecular axis (*10*), but such barrier-free unrestricted rotation cannot be powered or con-

trolled. The rotation of a dipolar rotor in a rotating electric field has been modeled (*11*). Examples in which control is possible are provided by the interlocked rings of catenanes that undergo circumrotation by passing through each other (*12*, *13*). However, machines with rotary motion about a rigid molecular axis, controlled by simple electron transfer processes or by photoexcitation, have not been previously reported.

The basis of the molecular device reported here has been known since the discovery (*14*) of the d⁷ Ni(III) and d⁶ Ni(IV) *commo*-bis-7,8-dicarbollyl metallocarboranes, denoted as **1T** (*15*) and **1C** (*16*) (Fig. 1), and their palladium analogs. These complexes are produced by the coordination of two dicarbollide ions (*17*) (Fig. 1, **2**) with a Ni(II) ion, followed by subsequent oxidation. The “sandwich” species may undergo rotary motion of the ligands with respect to each other. This is analogous to the well-known metallocenes (*18*), but those have rotational barriers only of 2 kcal/mol (*19*.) The present metallocarboranes have barriers about three times as large, leading to temperature invariance in their nuclear magnetic resonance (NMR) spectra.

The presence of two adjacent CH vertices in the bonding face of **2** introduces localized regions of reduced negative charge (*20*) and an antipodal concentration of negative charge. The resulting interligand interaction leads to a *trans* configuration (*15*, *17*, *21*) (such as in **1T**) in most examples of *commo*-bis-7,8-dicarbollyl metallocarboranes. One of the few exceptions is the Ni(IV) species (**1C**), which is *cisoid*, with its pairs of carbon vertices on the same side of the molecule (*14*, *15*). Nickel rarely appears in the formal +4 oxidation state in inorganic structures (*22*) and never in organometallic compounds, thereby making **1C** quite unusual.

The interconversion of the **1T** and **1C** geometries when the nickel oxidation state is changed provides the basis for the controlled, rotational, oscillatory motion and can be achieved electrochemically, by redox reactions, or photochemically. Thus, an oscillatory molecular rotor, providing useful work on the molecular scale, is plausible, based on the

controlled $4\pi/5$ rotation of the dicarbollide ligands coupled to ancillary structures.

Both **1T** and **1C** maintain their solid-state structures (15, 16) in solution, as shown by the large 6.16-D dipole moment measured (14) for **1C** in cyclohexane solution and by the electronic and infrared spectra of **1T** measured in both solution and the solid state. We demonstrated the quantitative reversibility of the **1T/1C** redox couple with reversible cyclic voltammograms [-0.66 V versus the standard calomel electrode (SCE)].

We show experimentally and theoretically that the **1C** and **1T** interconversion acts as a rotating molecular machine. Photoexcitation induces geometrical changes similar to those caused by electrochemical reduction. Reduction places an electron in the lowest unoccupied molecular orbital (LUMO); photoexcitation removes an electron from the highest occupied molecular orbital (HOMO) and places it in the LUMO.

Direct spectroscopic evidence for photon-driven rotation is provided by resonance Raman spectroscopy (23–25). The largest distortions are associated with the very intense low-frequency bands at 63 cm^{-1} and 198 cm^{-1} . On the basis of density functional theory (DFT) calculations, the 63 cm^{-1} band is associated with the rotational motion (i.e., a dicarbollide-dicarbollide torsional normal coordinate), and the 198 cm^{-1} band is assigned as a metal-dicarbollide elongation (i.e., a symmetric stretch along the ligand-metal-ligand normal coordinate). These distortions, excited by population of the lowest energy excited electronic state, produce a corkscrew motion that simultaneously rotates the ligands and elongates the metal-ligand bonds. Excited-state DFT calculations show that the minimum energy corresponds to a rotation of 130° , which is near to that of the ground-state *transoid* configuration of the Ni(III) bis-dicarbollide species.

The luminescence spectrum of Ni(IV) provided further supporting evidence for photon-driven rotation. The emission band was markedly red-shifted from the corresponding absorption band and contains a large ($>2000\text{ cm}^{-1}$) energy gap (Fig. 2). This is consistent with a process wherein the molecule absorbs a photon, relaxes to its minimum energy configuration in the excited state by rotating, and then emits from this new configuration (26).

To understand the rotatory operation of the molecule (Fig. 1), DFT (27, 28) was used to calculate the molecular and orbital energies of the unsubstituted (where hydrogen is attached to the four carbon vertices: $R^1, R^2, R^3,$ and R^4 represent H) species as a function of the rotational angle α . Time-dependent DFT (28) was used to compute the vertical electronic excitation. Hartree-Fock calculations (29) yielded qualitatively similar results. The energetics driving the machine are shown in Fig. 3. The Ni(IV) species has a stable *cisoid* position (144°) and a maximum at the *transoid* position (0°), whereas Ni(III) is stable at the *transoid*

Fig. 1. Illustration of rotor configurations of Ni(IV) (**1C**) and Ni(III) (**1T**) and the structural modules from which they are constructed. Structure **1T** is defined with rotation angle $\alpha = 0^\circ$. The diastereomers obtained by substitution of R for H at a single carbon vortex of the 7,8 ligands are *meso* ($R^1 = R^4 = \text{H}, R^2 = R^3 = \text{substituent}$) and *dl* ($R^1 = R^3 = \text{H}, R^2 = R^4 = \text{substituent}$ and $R^1 = R^3 = \text{substituent}, R^2 = R^4 = \text{H}$; *d* and *l* assignments are arbitrary).

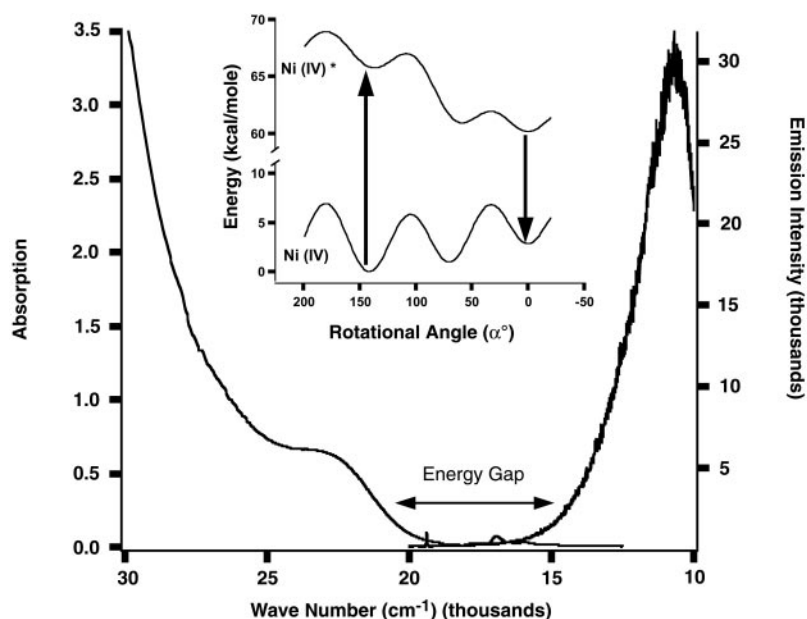


Fig. 2. Absorption (left) and emission (right) spectra of the Ni(IV) compound with $R^1 = R^2 = R^3 = R^4 = \text{H}$. Inset: The calculated energies of the ground and excited electronic states as a function of rotation angle. After absorption of a photon (left arrow), the molecule rotates and then luminesces (right arrow).

configuration (0°). On excitation of Ni(IV), the excited-state potential has a minimum at 0° (Fig. 2, inset). The operation of the molecular machine can also be understood in terms of the orbital-energies Walsh correlation diagram for the Ni(IV) species (Fig. 3), which shows that the HOMO has a minimum at the *cisoid* configuration and a maximum near the *transoid* configuration. In the minimum energy configuration, this MO is bonding between the two rings' dicarbollide ligands. The strongly antibonding LUMO has a nodal plane through the nickel atom, bisecting the metal axle.

Electrochemical reduction of the Ni(IV) compound placed an electron in the LUMO. A portion of the driving force for the rotation is explained by the stabilization of this orbital as the ligands rotate to the *transoid* configuration. The calculated total energy of the reduced molecule decreased by ~ 4

kcal/mol during this 144° rotation. The intrinsic uncertainties in the methods of calculation are a few kcal/mol. The calculated energy change is an underestimate; experimentally (with NMR), only a single static configuration was observed. A large average torque of $8 \times 10^3\text{ Nm/mol}$ was associated with this rotatory motion. Oxidation of the Ni(III) compound to its Ni(IV) counterpart required $\sim 64\text{ kcal/mol}$, which was followed by a recovery of $\sim 2.8\text{ kcal/mol}$ on rotation to the Ni(IV) ground state, giving an efficiency of $\sim 4.2\%$ (not including solvation effects). Photoexcitation of the Ni(IV) compound removed an electron from the HOMO and placed it in the LUMO. This excitation provides a portion of the driving force for rotation, which is related to that resulting from electrochemical placement of an electron in the LUMO. An additional increment of driving force resulted from the

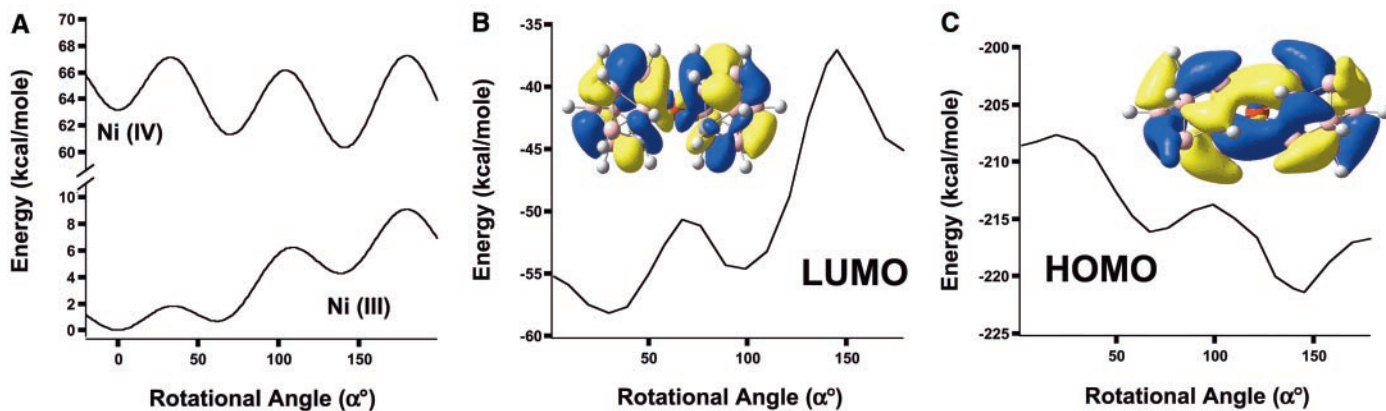


Fig. 3. Calculated energies as a function of rotation angle for $R^1 = R^2 = R^3 = R^4 = H$. (A) Total energies of the Ni(III) and Ni(IV) compounds. The minimum in the Ni(III) energy occurs at the *transoid* and that in Ni(IV) at the *cisoid* configuration. (B and C) Energies of the (B) LUMO and (C) HOMO of

the Ni(IV) compound. The probability contours of the orbitals are also shown. The minimum energy of the HOMO corresponds to the *cisoid* geometry and that of the LUMO to the *transoid* configuration, illustrating why the molecule rotates when the LUMO becomes occupied.

loss of the electron from the HOMO with its minimum at the *cisoid* configuration. In addition, placement of the electron in the antibonding LUMO is expected to cause an increase in the ligand-ligand distance, as is evidenced by the strong enhancement of the symmetric stretching mode in the resonance Raman spectrum. The time-dependent DFT calculation corroborates these results in terms of the total energy of the excited states.

Although the parent Ni(III)/IV) metallacarborane couple (**1T/1C**; where R^1, R^2, R^3 , and R^4 are H) cannot effectively rotate more than $4\pi/5$ about its rotational axis, the direction of this rotation should depend on stereochemical interactions of organic substituents if present on the carbon vertices (Fig. 1). If each of the dicarbollide ligands has one CH (R is H) and one CR (R is an organic substituent such as methyl, CH_3), the resulting ligand asymmetry will produce two diastereomeric sets of substituted Ni(III)/Ni(IV) couples. These diastereomers are designated *dl* (one enantiomer of arbitrary configuration selected for discussion with R^1 and R^3 as H and R^2 and R^4 as an organic substituent) and *meso* (R^1 and R^4 as H and R^2 and R^3 as an organic substituent).

One-electron oxidation of the depicted Ni(III) enantiomer (**1T**) allowed the upper dicarbollide ligand to rotate either clockwise or counterclockwise with respect to the lower dicarbollide ligand. A $4\pi/5$ rotation in a clockwise direction achieved the *cisoid* Ni(IV) structure **1C**. An additional clockwise $2\pi/5$ motion generated an isomeric *cisoid* structure with the R groups of the two ligands in close contact. This interligand R-R repulsion would destabilize this $6\pi/5$ rotational isomer with respect to the first-formed $4\pi/5$ isomer. Counterclockwise rotation of the upper ligand could only have proceeded to the extent of $2\pi/5$ before the two substituent R groups come into close contact, thereby preventing further rotation and the formation of the stabilized **1C** *cisoid* structure. Thus, the ground state-to-ground state rotation

of the selected enantiomer, resulting from conversion of Ni(III) to Ni(IV), occurred by the $4\pi/5$ clockwise rotation pathway. The enantiomer of this Ni(IV) species would preferentially rotate counterclockwise. Both processes would be reversed upon one-electron reduction of the corresponding Ni(IV) enantiomers. Oxidation of the *meso*-Ni(III) isomer provides equal probability of $4\pi/5$ rotation in a clockwise or counterclockwise direction. Thus, no preferential direction of rotation is possible, as expected for an achiral reactant proceeding to an achiral product. Reduction (oxidation), with motion, of the *d*- and *l*- enantiomers of **1C** (**1T**) should proceed at different rates with an enantiomerically enriched chiral reductant (oxidant).

This metallacarborane “nanowager,” when actuated by electrical or light energy, underwent large-amplitude rotational motion and thus exhibited two important criteria for bottom-up construction of a nanomachine. If one of the dicarbollide ligands were covalently bonded to a surface to prevent its rotation and the unencumbered ligand were made to rotate, a complete machine could be synthesized. If two or more individual motors with identical rotational properties are linked to each other along their rotational axes, the resulting “ganged” rotor assembly will be capable of delivering unidirectional rotation in multiples of $4\pi/5$, by successive oxidation or reduction of the component nickel centers. Potential applications of the circular motion include modifying, on command, the properties of a surface or molecule to which the device is attached and blocking and opening specific regions on a surface, such as pores or reactive sites. Operation of the nanowager is not limited to physiological pH in aqueous media; it could function in a variety of environments, including organic and inorganic liquids, gases, and vacuum.

References and Notes

1. J. T. Finer, R. M. Simmons, J. A. Spudick, *Nature* **368**, 113 (1994).
2. J. D. Huang *et al.*, *Nature* **397**, 267 (1999).

3. P. Boyer, *Biochim. Biophys. Acta* **1140**, 215 (1993).
4. Y. Sambongi *et al.*, *Science* **286**, 1722 (1999).
5. R. Yasuda, H. Naji, K. Kinoshita Jr., M. Yoshida, *Cell* **93**, 1117 (1998).
6. V. Balzani, A. Credi, F. M. Raymo, F. J. Stoddart, *Angew. Chem. Int. Ed. Engl.* **39**, 3348 (2000).
7. P. L. Anelli, N. Spencer, J. F. Stoddart, *J. Am. Chem. Soc.* **113**, 5131 (1991).
8. D. A. Leigh, A. Troisi, F. Zerbetto, *Angew. Chem. Int. Ed.* **39**, 350 (2000).
9. S. Chia, J. Cao, J. F. Stoddart, J. I. Zink, *Angew. Chem. Int. Ed.* **40**, 2447 (2001).
10. T. C. Bedard, J. S. Moore, *J. Am. Chem. Soc.* **117**, 10662 (1995).
11. J. Vacek, H. Michl, *Proc. Natl. Acad. Sci. U.S.A.* **98**, 5481 (2001).
12. V. Balzani *et al.*, *J. Org. Chem.* **65**, 1924 (2000).
13. M. Asakawa *et al.*, *J. Org. Chem.* **62**, 26 (1997).
14. L. F. Warren Jr., M. F. Hawthorne, *J. Am. Chem. Soc.* **92**, 1157 (1970).
15. F. V. Hansen, R. G. Hazell, C. Hyatt, G. D. Stucky, *Acta Chem. Scand. A* **27**, 1210 (1973).
16. D. St. Clair, A. Zalkin, D. H. Templeton, *J. Am. Chem. Soc.* **92**, 1173 (1970).
17. M. F. Hawthorne, G. B. Dunks, *Science* **178**, 462 (1972).
18. J. E. Huheey, E. R. A. Keiter, R. L. Keiter, *Inorganic Chemistry* (Harper Collins, New York, ed. 4, 1993).
19. R. K. Bohn, A. Haaland, *J. Organomet. Chem.* **5**, 470 (1966).
20. R. G. Adler, M. F. Hawthorne, *J. Am. Chem. Soc.* **92**, 6174 (1970).
21. M. F. Hawthorne *et al.*, *J. Am. Chem. Soc.* **90**, 879 (1968).
22. F. A. Cotton, G. Wilkinson, C. A. Murillo, M. Bochmann, *Advanced Inorganic Chemistry* (Wiley, New York, ed. 5, 1999), pp. 847–848.
23. K. S. K. Shin, J. I. Zink, *Inorg. Chem.* **28**, 4358 (1989).
24. E. J. Heller, R. L. Sundberg, D. Tannor, *J. Phys. Chem.* **86**, 1822 (1982).
25. J. I. Zink, K. S. K. Shin, in *Advances in Photochemistry*, D. Volman, G. Hammond, D. Neckers, Eds. (Wiley, New York, 1991), vol. 16, pp. 119–214.
26. D. M. Preston, W. Guntner, A. Lechner, G. Gliemann, J. I. Zink, *J. Am. Chem. Soc.* **110**, 5628 (1988).
27. *Gaussian 98*, Revision A.9; Frisch *et al.* (Gaussian, Pittsburgh, PA, 1998).
28. *Q-Chem 2.0*, J. Kong *et al.*, *J. Comput. Chem.* **21**, 1532 (2000).
29. *Jaguar 4.1*, Schroedinger, Portland, OR (2000).
30. Supported by NSF grant nos. CHE-0111718 (M.F.H.), CHE-0315292 (D.N.), and CHE-0102623 (J.I.Z.); an Israel Science Foundation grant (R.B.); and NSF equipment grant nos. CHE-9871332, CHE-9610080, CHE-9808175, CHE-0078299, and CHE-9974928 for NMR and mass spectrometers.

20 November 2003; accepted 3 February 2004

This copy is for your personal, non-commercial use only.

If you wish to distribute this article to others, you can order high-quality copies for your colleagues, clients, or customers by [clicking here](#).

Permission to republish or repurpose articles or portions of articles can be obtained by following the guidelines [here](#).

The following resources related to this article are available online at www.sciencemag.org (this information is current as of August 29, 2015):

Updated information and services, including high-resolution figures, can be found in the online version of this article at:

<http://www.sciencemag.org/content/303/5665/1849.full.html>

This article **cites 25 articles**, 3 of which can be accessed free:

<http://www.sciencemag.org/content/303/5665/1849.full.html#ref-list-1>

This article has been **cited by** 103 article(s) on the ISI Web of Science

This article has been **cited by** 4 articles hosted by HighWire Press; see:

<http://www.sciencemag.org/content/303/5665/1849.full.html#related-urls>

This article appears in the following **subject collections**:

Chemistry

<http://www.sciencemag.org/cgi/collection/chemistry>